TE-Mode Scattering from Two Junctions in H-Plane Waveguide

Jae W. Lee and Hyo J. Eom

Abstract—**An analytic series solution for TE-mode scattering from two junctions in the H-plane waveguide is obtained. A Fourier-transform technique is applied to express the scattered field in the spectral domain in terms of parallel-plate waveguide modes. The boundary conditions are enforced to obtain simultaneous equations for the transmitted field. The simultaneous equations are solved to obtain the transmission and reflection coefficients in simple series forms. Comparisons between our solution and other existing results show excellent agreements. The behaviors of scattering from two junctions are studied in terms of frequency and junction geometry. The obtained analytic solutions are simple series so that they are very efficient for numerical computation.**

I. Introduction

THE problem of the rectangular waveguide T-junction has been extensively studied by many investigators [1]–[3] since Marcuvitz [4] first obtained the approximate solution. Recently, we have obtained analytic series solutions to the problems of the E- and H-plane T-junctions [5, 6] utilizing the Fourier transform and the mode matching method. The motivation of the present paper is to show the same techniques used in [5], [6] can be applied to the problem of scattering from two junctions in the H-plane waveguide. For the sake of completeness, we assume that two junctions are either short- or open-circuited. The organization of the paper is as follows: In Section II, the fields are represented in the spectral domain, and the boundary conditions are used in Section III to formulate the simultaneous equations for the field coefficients. In Section IV, the simultaneous equations are solved to represent the field coefficients in series form. In Section V, the analytic expression for the transmission and reflection coefficients are derived. In Section VI, the numerical computations are performed to investigate the scattering behaviors. A brief summary is given in Section VII.

II. Field Representations

Two junctions in the H-plane waveguide are shown in Fig. 1. A TE$_s$-mode $E_y^i(x,z)$, which is transverse-electric (TE) to the x-axis, is incident on the junctions. Here, time factor $\exp(-i\omega t)$ is suppressed and the medium wave number is $k_1(=2\pi/\lambda=\omega\sqrt{\mu\epsilon})$. In region (I) $(-b<z<0)$ the total electric field consists of the incident and scattered fields,

Manuscript received March 4, 1993; revised June 15, 1993.

The authors are with the Department of Electrical Engineering, Korea Advanced Institute of Science and Technology, 373-1, Kusong Dong, Yusung Gu, Taejon, Korea.

IEEE Log Number 9216053.

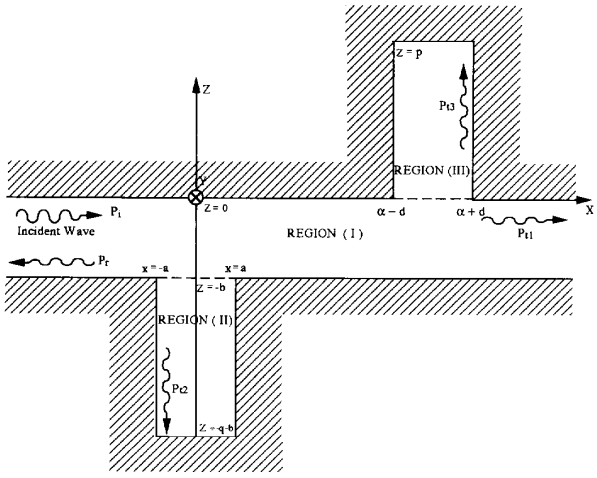

Fig. 1. Scattering Geometry of Two Junctions in H-Plane Waveguide.

$E_y^i(x,z)$ and $E_y^{\mathrm{I}}(x,z)$.

$$E_y^i(x,z)=e^{ik_{xs}x}\sin k_{zs}(z+b) \tag{1}$$

$$E_y^{\mathrm{I}}(x,z)=1/(2\pi)\int_{-\infty}^{\infty}[\tilde{E}_y^{s+}(\zeta)e^{i\kappa_1 z}+\tilde{E}_y^{s-}(\zeta)e^{-i\kappa_1 z}]e^{-i\zeta x}d\zeta \tag{2}$$

where

$$\kappa_1=\sqrt{k_1^2-\zeta^2} \tag{3}$$

$$k_{zs}=\frac{s\pi}{b} \qquad s:\ \text{integer} \tag{4}$$

$$k_{xs}=\sqrt{k_1^2-k_{zs}^2}. \tag{5}$$

In region (II) $(-a<x<a, -q-b<z<-b)$ the transmitted field may be represented as

$$E_y^{\mathrm{II}}(x,z)=\sum_{m=1}^{\infty}c_m\sin a_m(x+a)Y_q(z) \tag{6}$$

where

$$a_m=m\pi/(2a) \tag{7}$$

$$\xi_m=\sqrt{k_1^2-a_m^2} \tag{8}$$

$$Y_q(z)=\begin{cases}e^{-j\xi_m z}\\ \sin\xi_m(z+b+q)\end{cases}\begin{matrix}\\ :\ \text{open-circuited}\ (q\to\infty)\\ :\ \text{short-circuited}\end{matrix} \tag{9}$$

$$Y_q'(z) = dY_q(z)/dz. \tag{10}$$

In region (III) $(\alpha - d < x < \alpha + d, 0 < z < p)$ the transmitted field is

$$E_y^{\mathrm{III}}(x,z) = \sum_{m=1}^{\infty} d_m \sin b_m(x-\alpha+d) X_p(z) \tag{11}$$

where
$$b_m = m\pi/(2d) \tag{12}$$
$$\eta_m = \sqrt{k_1^2 - b_m^2} \tag{13}$$
$$X_p(z) = \begin{cases} e^{j\eta_m z} & : \text{open-circuited } (p \to \infty) \\ \sin \eta_m(z-p) & : \text{short-circuited} \end{cases} \tag{14}$$
$$X_p'(z) = dX_p(z)/dz. \tag{15}$$

III. Matching Boundary Conditions

To determine unknown coefficient c_m and d_m, it is necessary to match the boundary conditions of tangential field continuities. The tangential electric field continuity at $z = -b$ yields

$$E_y^{\mathrm{I}}(x,-b) = E_y^{\mathrm{II}}(x,-b) \quad |x| < a \tag{16}$$
$$= 0 \quad |x| > a. \tag{17}$$

Taking the Fourier transform of both sides, we get

$$\int_{-\infty}^{\infty} E_y^{\mathrm{I}}(x,-b) e^{i\zeta x} dx = \int_{-a}^{a} E_y^{\mathrm{II}}(x,-b) e^{i\zeta x} dx. \tag{18}$$

Similarly the tangential electric field continuity at $z = 0$ gives

$$\int_{-\infty}^{\infty} E_y^{\mathrm{I}}(x,0) e^{i\zeta x} dx = \int_{\alpha-d}^{\alpha+d} E_y^{\mathrm{III}}(x,0) e^{i\zeta x} dx. \tag{19}$$

Substituting (6) into (18) and performing integration with respect to x, we obtain

$$\tilde{E}_y^{s+}(\zeta) e^{-i\kappa_1 b} + \tilde{E}_y^{s-}(\zeta) e^{i\kappa_1 b} = \sum_{m=1}^{\infty} c_m Y_q(-b) \frac{a_m}{(\zeta^2 - a_m^2)} \times [e^{i\zeta a}(-1)^m - e^{-i\zeta a}]. \tag{20}$$

Similarly from (11) and (19),

$$\tilde{E}_y^{s+}(\zeta) + \tilde{E}_y^{s-}(\zeta) = \sum_{m=1}^{\infty} d_m X_p(0) \frac{b_m e^{i\zeta\alpha}}{(\zeta^2 - b_m^2)} [e^{i\zeta d}(-1)^m - e^{-i\zeta d}]. \tag{21}$$

The tangential magnetic field continuity along $(-a < x < a, z = -b)$ gives

$$k_{zs} e^{ik_{xs}x} + \frac{1}{2\pi} \int_{-\infty}^{\infty} i\kappa_1 [\tilde{E}_y^{s+}(\zeta) e^{-i\kappa_1 b} - \tilde{E}_y^{s-}(\zeta) e^{i\kappa_1 b}] e^{-i\zeta x} d\zeta = \sum_{m=1}^{\infty} c_m \sin a_m(x+a) Y_q'(-b). \tag{22}$$

Similarly the tangential magnetic field continuity along $(\alpha - d < x < \alpha + d, z = 0)$ gives

$$k_{zs} e^{ik_{xs}x} \cos(k_{zs}b) + \frac{1}{2\pi} \int_{-\infty}^{\infty} i\kappa_1 [\tilde{E}_y^{s+}(\zeta) - \tilde{E}_y^{s-}(\zeta)] e^{-i\zeta x} d\zeta = \sum_{m=1}^{\infty} d_m \sin b_m(x-\alpha+d) X_p'(0). \tag{23}$$

We solve (20) and (21) for $\tilde{E}_y^{s+}(\zeta)$ and $\tilde{E}_y^{s-}(\zeta)$. Substituting $\tilde{E}_y^{s+}(\zeta)$ and $\tilde{E}_y^{s-}(\zeta)$ into (22) and (23), we obtain

$$\begin{aligned} k_{zs} e^{ik_{xs}x} &- \sum_{m=1}^{\infty} c_m Y_q(-b) \frac{a_m}{2\pi} \\ &\times \int_{-\infty}^{\infty} \kappa_1 \cot(\kappa_1 b) K_m^a(a) e^{-i\zeta x} d\zeta \\ &+ \sum_{m=1}^{\infty} d_m X_p(0) \frac{b_m}{2\pi} \int_{-\infty}^{\infty} \frac{\kappa_1 e^{i\zeta\alpha}}{\sin(\kappa_1 b)} \\ &\times K_m^d(b) e^{-i\zeta x} d\zeta \\ &= \sum_{m=1}^{\infty} c_m \sin a_m(x+a) Y_q'(-b) \end{aligned} \tag{24}$$

$$\begin{aligned} k_{zs} e^{ik_{xs}x} \cos(k_{zs}b) &- \sum_{m=1}^{\infty} c_m Y_q(-b) \frac{a_m}{2\pi} \\ &\times \int_{-\infty}^{\infty} \frac{\kappa_1}{\sin(\kappa_1 b)} K_m^a(a) e^{-i\zeta x} d\zeta \\ &+ \sum_{m=1}^{\infty} d_m X_p(0) \frac{b_m}{2\pi} \int_{-\infty}^{\infty} \kappa_1 \cot(\kappa_1 b) e^{i\zeta\alpha} \\ &\times K_m^d(b) e^{-\zeta x} d\zeta \\ &= \sum_{m=1}^{\infty} d_m \sin b_m(x-\alpha+d) X_p'(0) \end{aligned} \tag{25}$$

where

$$K_u^w(\nu) = \frac{(-1)^u e^{i\zeta w} - e^{-i\zeta w}}{\zeta^2 - \nu_u^2} \tag{26}$$
$$u = m, n \tag{27}$$
$$\nu = a, b \tag{28}$$
$$w = a, d. \tag{29}$$

IV. Determination of c_m and d_m

Note that (24) and (25) constitute the simultaneous equations for c_m and d_m. Multiplying (24) by $\sin a_n(x+a)$ and integrating with respect to x from $-a$ to a, we get

$$\begin{aligned} \frac{k_{zs} a_n}{k_{xs}^2 - a_n^2} &[(-1)^n e^{ik_{xs}a} - e^{-ik_{xs}a}] \\ &= \sum_{m=1}^{\infty} c_m Y_q(-b) \frac{a_m a_n}{2\pi} I_{1nm} - \sum_{m=1}^{\infty} d_m X_p(0) \frac{b_m a_n}{2\pi} I_{2nm} \\ &+ c_n a Y_q'(-b) \delta_{nm} \end{aligned} \tag{30}$$

where

$$I_{1nm} = \int_{-\infty}^{\infty} \kappa_1 cot(\kappa_1 b) K_m^a(a) K_n^{-a}(a) ds \tag{31}$$

$$I_{2nm} = \int_{-\infty}^{\infty} \frac{\kappa_1 e^{j\zeta\alpha}}{\sin(\kappa_1 b)} K_m^d(b) K_n^{-a}(a) ds. \tag{32}$$

Utilizing the technique of the contour integration, we evaluate where

$$I_{1nm} = \begin{cases} 0 & \text{when } n+m = \text{ odd} \\ h_m \delta_{nm} + r_{nm} & \text{when } n+m = \text{ even} \end{cases} \tag{33}$$

$$I_{2nm} = g_m \delta_{nm} \Delta + f_{nm} \tag{34}$$

where

$$\Delta = \begin{cases} 1 & \text{when } d = a \text{and } \alpha\ 0 \\ 0 & \text{otherwise} \end{cases} \tag{35}$$

$$B_m = -\pi[|d-a|e^{is}|d-a| - (-1)^m |d+a|e^{is}|d+a|] \tag{36}$$

$$h_m = \frac{2\pi a \xi_m}{a_m^2 \tan(\xi_m b)} \tag{37}$$

$$g_m = \frac{B_m \eta_m}{b_m^2 \sin(\eta_m b)} \tag{38}$$

$$r_{nm} = \sum_{l=1}^{\infty} 2\cos(1\pi) T_{\xi\xi}[1 - (-1)^m e^{iz\sqrt{ki^2 - (l\pi/b)^2}} \tag{39}$$

$$\begin{aligned} f_{nm} &= \sum_{l=1}^{\infty} T_{\eta\xi}[(-1)^{m+n} e^{i\zeta|d-a+\alpha|} - (-1)^m e^{i\zeta|d+a+\alpha|} \\ &\quad - (-1)^n e^{i\zeta|\alpha-a-d|} + e^{i\zeta|\alpha+a-d|}]\big|_s \\ &= \sqrt{ki^2 - (e\pi/b)^2} \end{aligned} \tag{40}$$

$$T_{u\nu} = \frac{-i2\pi(l\pi/b)^2}{\sqrt{k_1^2 - (l\pi/b)^2} b[u_m^2 - (l\pi/b)^2][\nu_n^2 - (l\pi/b)^2]\cos(l\pi)} \tag{41}$$

$$u, \nu = \xi, \eta. \tag{42}$$

Multiplying (24) by $\sin b_n(x - \alpha + d)$ and integrating the both sides with respect to x from $\alpha - d$ to $\alpha + d$, we get

$$\begin{aligned} &\frac{k_{zs}\cos(k_{zs}b) b_n e^{ik_{xs}\alpha}}{k_{xs}^2 - b_n^2}[(-1)^n e^{ik_{xs}d} - e^{-ik_{xs}d}] \\ &= \sum_{m=1}^{\infty} c_m Y_q(-b) \frac{a_m b_n}{2\pi} I_{3nm} - \sum_{m=1}^{\infty} d_m X_p(0) \frac{b_m b_n}{2\pi} I_{4nm} \\ &\quad + d_n d X_p'(0) \delta_{nm} \end{aligned} \tag{43}$$

where

$$I_{3nm} = \int_{-\infty}^{\infty} \frac{\kappa_1 e^{i\zeta\alpha}}{\sin(\kappa_1 b)} K_m^a(a) K_n^{-d}(b) ds \tag{44}$$

$$I_{4nm} = \int_{-\infty}^{\infty} \kappa_1 \cot(\kappa_1 b) K_m^d(b) K_n^{-d}(b) ds \tag{45}$$

I_{3nm} and I_{4nm} are evaluated to give

$$I_{3nm} = g_m \delta_{nm} \Delta + t_{nm} \tag{46}$$

$$I_{4nm} = \begin{cases} h_m \delta_{nm} + z_{nm} & \text{when } n+m = \text{ even} \\ 0 & \text{when } n+m = \text{odd} \end{cases} \tag{47}$$

where

$$z_{nm} = \sum_{l=1}^{\infty} 2\cos(l\pi) T_{\eta\eta} 1 - (-1)^m e^{i2\sqrt{ki^2 - (l\pi/b)^2}} \tag{48}$$

$$\begin{aligned} t_{nm} &= \sum_{l=1}^{\infty} T_{\xi\eta}[(-1)^{m+n} e^{i\zeta|-d+a-\alpha|} - (-1)^m e^{i\zeta|d+a-\alpha|} \\ &\quad - (-1)^n e^{i\zeta|-\alpha-a-d|} + e^{i\zeta|-\alpha-a+d|}]\big|_s \\ &= \sqrt{ki^2 - (e\pi/b)^2}. \end{aligned} \tag{49}$$

Substituting (33), (34), (46), and (47) into (30) and (43), we obtain

$$\begin{bmatrix} \Psi_1 & \Psi_2 \\ \Psi_3 & \Psi_4 \end{bmatrix} \begin{bmatrix} C \\ D \end{bmatrix} = \begin{bmatrix} \Gamma_1 \\ \Gamma_2 \end{bmatrix} \tag{50}$$

where C and D are column vectors consisting of elements c_m and d_m, respectively, and $\Psi_1, \Psi_2, \Psi_3, \Psi_4, \Gamma_1$ and Γ_2 are matrices whose elements are

$$\begin{aligned} \psi_{1,nm} &= a\left[\frac{\xi_n Y_q(-b)}{\tan\xi_n b} + Y_q'(-b)\right]\delta_{nm} + Y_q(-b)\frac{a_n a_m r_{nm}}{2\pi} \\ &\equiv \psi_1^{(0)}\delta_{mn} + \psi_1^{(1)} \end{aligned} \tag{51}$$

$$\begin{aligned} \psi_{2,nm} &= -X_p(0)\frac{B_m \xi_n \Delta}{2\sin\xi_n b}\delta_{nm} - X_p(0)\frac{b_m a_n f_{nm}}{2\pi} \\ &\equiv \psi_2^{(0)}\delta_{mn} + \psi_2^{(1)} \end{aligned} \tag{52}$$

$$\begin{aligned} \psi_{3,nm} &= Y_q(-b)\frac{B_m \xi_n \Delta}{2\sin\xi_n b}\delta_{nm} + Y_q(-b)\frac{a_m b_n}{2\pi} t_{nm} \\ &\equiv \psi_3^{(0)}\delta_{mn} + \psi_3^{(1)} \end{aligned} \tag{53}$$

$$\begin{aligned} \psi_{4,nm} &= -d\left[\frac{\eta_n X_p(0)}{\tan\eta_n b} - X_p'(0)\right]\delta_{nm} - X_p(0)\frac{b_m b_n z_{nm}}{2\pi} \\ &\equiv \psi_4^{(0)}\delta_{mn} + \psi_4^{(1)} \end{aligned}$$

$$\gamma_{1n} = \frac{k_{zs} a_n[(-1)^n e^{ik_{xs}a} - e^{-ik_{xs}a}]}{k_{xs}^2 - a_n^2} \tag{55}$$

$$\gamma_{2n} = \frac{k_{zs} b_n \cos(k_{zs}b) e^{ik_x\alpha}[(-1)^n e^{ik_{xs}d} - e^{-ik_{xs}d}}{k_{xs}^2 - b_n^2}. \tag{56}$$

Solving (50) for C and D,

$$C = (\Psi_1 - \Psi_2\Psi_4^{-1}\Psi_3)^{-1}(\Gamma_1 - \Psi_2\Psi_4^{-1}\Gamma_2) \tag{57}$$

$$D = (\Psi_2 - \Psi_1\Psi_3^{-1}\Psi_4)^{-1}(\Gamma_1 - \Psi_1\Psi_3^{-1}\Gamma_2). \tag{58}$$

In high-frequency regime ($\omega \to \infty$, i.e., $k_1 b \to \infty$) and $\Delta = 0, c_m$ and d_m reduce to the Kirchhoff solution in closed forms,

$$c_m \approx \gamma_{1m}/\psi_1^{(0)} \tag{59}$$

$$d_m \approx \gamma_{2m}/\psi_4^{(0)}. \tag{60}$$

V. Derivation of Reflection and Transmission Coefficients

It is of interest to obtain the reflection and transmission coefficients in analytic forms. In region (I) the total scattered field is given by (2)

where $$\tilde{E}_y^{s+}(\zeta) = \frac{-1}{2i\sin\kappa_1 b}\left[\sum_{m=1}^{\infty} c_m a_m Y_q(-b) K_m^a(a) - e^{i\kappa_1 b}\sum_{m=1}^{\infty} d_m b_m X_p(0) e^{i\zeta\alpha} K_m^d(b)\right] \tag{61}$$

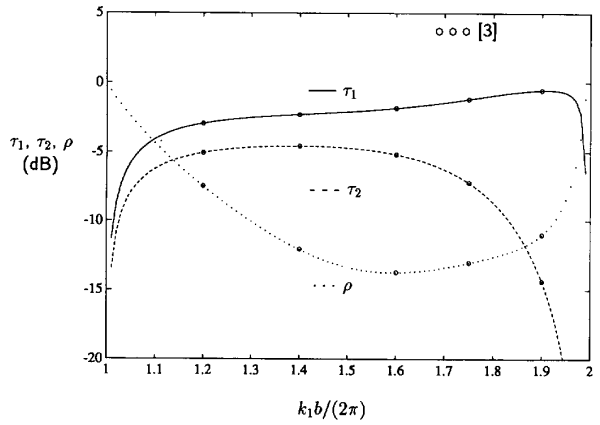

Fig. 2. Comparision of Transmission (τ_1 and τ_2)and Reflection Coefficients (ρ)versus Normalized Frequency ($k_1 b/(2\pi)$) ($b/a = 4$, $d/a = 1$, $p = q = \infty$, $s = 2$, $\alpha = 0$).

$$\tilde{E}_y^{s-}(\zeta) = \frac{1}{2i \sin \kappa_1 b}\left[\sum_{m=1}^{\infty} c_m a_m Y_q(-b) K_m^a(a) - e^{-i\kappa_1 b}\sum_{m=1}^{\infty} d_m b_m X_p(0) e^{i\zeta\alpha} K_m^d(b)\right]. \tag{62}$$

By use of residue calculus, we evaluate total transmitted and reflected fields at $x = \pm\infty$ in region (I),

$$E_y^{\mathrm{I}}(\pm\infty, z) = \sum_v L_v^{\pm} \sin k_{zv}(z+b) e^{\pm i k_{xv} x} \tag{63}$$

where

$$1 \le v < \frac{k_1 b}{\pi} \quad v : \text{integer } (1, 2, 3, \ldots) \tag{64}$$

$$k_{zv} = \frac{v\pi}{b} \tag{65}$$

$$k_{xv} = \sqrt{k_1^2 - k_{zv}^2} \tag{66}$$

$$L_v^{\pm} = \sum_{m=1}^{\infty} i c_m Y_q(-b) \frac{a_m k_{zv}}{k_{xv} b (k_{xv}^2 - a_m^2)} \left[e^{\mp i k_{xv} a}(-1)^m - e^{\pm i k_{xv} a}\right] - \sum_{m=1}^{\infty} i d_m X_p(0) \frac{b_m k_{zv} e^{\mp i k_{xv}\alpha}}{k_{xv} b (-1)^v (k_{xv}^2 - b_m^2)} \times \left[e^{\pm i k_{xv} d}(-1)^m - e^{\mp i k_{xv} d}\right]. \tag{67}$$

Let the time-averaged incident, transmitted, and reflected powers be denoted by P_i, P_{t1}, P_{t2} and P_r as shown in Fig. 1, then the transmission (τ_1, τ_2, and τ_3) and reflection (ρ) coefficients are

$$\tau_1 = P_{t1}/P_i = |1 + L_s^+|^2 + \frac{1}{k_{xs}} \sum_{v \neq s} k_{xv} |L_v^+|^2 \tag{68}$$

$$\rho = P_r/P_i = \frac{1}{k_{xs}} \sum_v k_{xv} |L_v^-|^2 \tag{69}$$

$$\tau_2 = P_{t2}/P_i = \frac{2a}{k_{xs} b} \sum_{m1} \xi_{m1} |c_{m1}|^2 \tag{70}$$

$$\tau_3 = P_{t3}/P_i = \frac{2d}{k_{xs} b} \sum_{m_2} \eta_{m2} |d_{m2}|^2 \tag{71}$$

where

$$1 \le m1 < \frac{2ak_1}{\pi} \quad m1 : \text{integer} \tag{72}$$

$$1 \le m2 < \frac{2dk_1}{\pi} \quad m2 : \text{integer} \tag{73}$$

$$1 \le v < \frac{k_1 b}{\pi} \quad v : \text{integer.} \tag{74}$$

VI. Numerical Evaluations

We first verify the numerical accuracy of our computation in Fig. 2 when the TE_2-mode is incident on the cross junction. Fig. 2 shows the comparision of our τ_1, τ_2, and ρ to the results of [3], confirming excellent agreements between two results. We next check the convergence rate of c_m and d_m by tabulating $|c_m Y_q(-b)|, |d_m X_p(0)|$, and their energy conservation characteristics $(\rho + \tau_1 + \tau_2)$ in Table I when $p = 0.2\lambda$ and $q = \infty$. Note, that our result in Table I satisfies the energy conservation check $|1.0 - (\rho + \tau_1 + \tau_2)| < 10^{-6}$ when six modes are used in the computation. Our computational experience shows that the number of modes m to be used for the evaluation of c_m in (57) must be at least $2ak_1/\pi$ to achieve the numerical accuracy. This means that the series expression c_m and d_m given in (57) is very fast convergent and numerically efficient. Fig. 3(a)-(c) show the behaviors of τ_1, τ_2, and ρ versus p, respectively when the TE_1 mode is incident on the T-junction with a short-circuited junction (i.e., shorting plunger). It is interesting to note that when $p = 0.27\lambda$ and $\alpha = -0.75\lambda$ the T-junction almost acts like an ideal power divider ($\tau_1 \approx \tau_2 \approx 0.49, \rho = 0.02$). Fig. 4 shows the behaviors of τ_1 versus the normalized frequency $k_1 b/\pi$ when the TE_1 mode is incident on two short-circuited junctions. It has been experimentally verified in [7] that the rectangular waveguide with a short-circuited junction can be used as a band-stop filter. In Fig. 4, we show the effects of the length (p) variation on the band-stop filter characteristics. When $p = 0$, our computation agrees with the result in [7]. As p increases, the center frequency of the band-stop filter tends to slightly decrease and its bandwidth becomes narrower. This implies that a simultaneous use of two short-circuited junctions in the rectangular waveguide enables us to realize a notch filter with a very high Q. Fig. 5 shows the behaviors of τ_1, τ_2, and ρ versus the normalized frequency $k_1 b/\pi$ when the TE_1 mode is incident on the H-plane cross-junction. There exist abrupt changes in τ_1, τ_2, and ρ whenever an inset of the new higher modes takes place at $k_1 b/\pi = 2, 3, \cdots$. It is seen that most of P_i is transmitted through the waveguide (i.e., $\tau_1 > 0.7$), indicating that the H-plane cross-junction can not be considered a useful power divider. We also evaluate scattering from two open-circuited junctions in the H-plane waveguide. Note that our solution is irrespective of α, different from cascading the solutions of two independent T-junction in [5]. This difference is attributed to the fact that cascading the solutions in [5] can not account for multiple reflections occurring between two junctions.

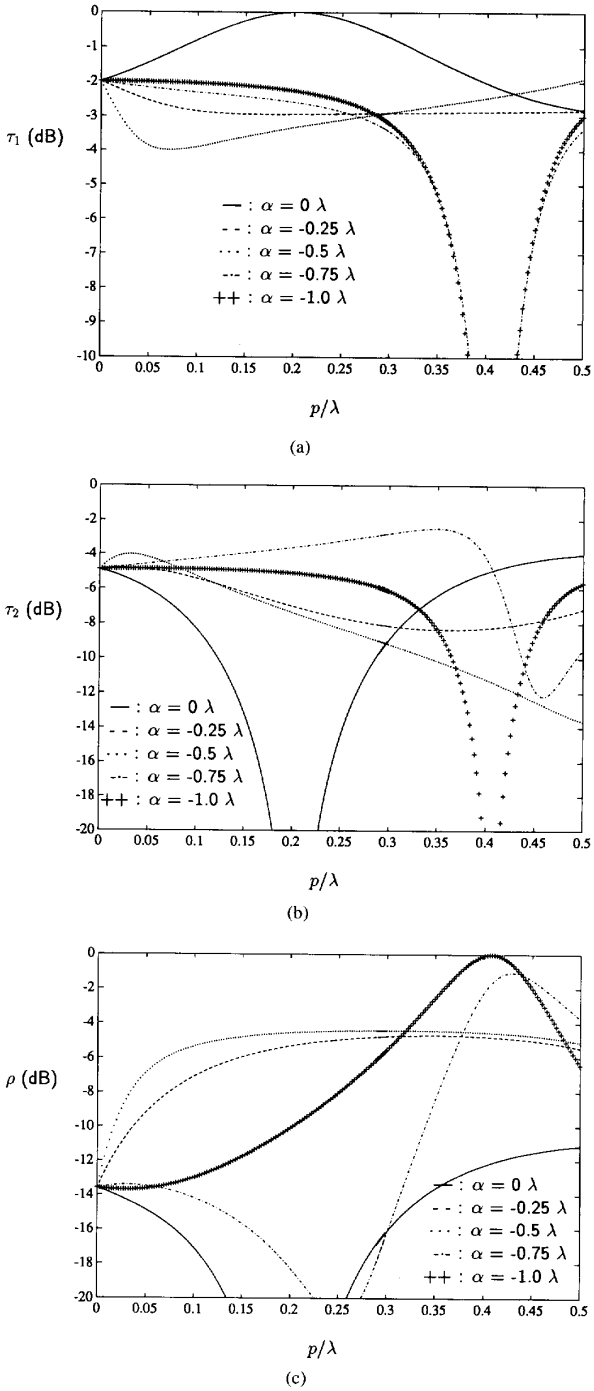

Fig. 3. Behaviors of TransmissionCoefficient (τ_1)versus p for Different $\alpha(b/a = 2, d/a = 1, q = \infty, s = 1, k_1 b/\pi = 1.55)$(b) Behaviors of Transmission Coefficient (τ_2)versus p for Different $\alpha(b/a = 2, d/a = 1, q = \infty, s = 1, k_1 b/\pi = 1.55)$(c) Behaviors of Reflection Coefficient (ρ)versus p for Different $\alpha(b/a = 2, d/a = 1, q = \infty, s = 1, k_1 b/\pi = 1.55)$.

VII. Conclusion

The problem of two junctions in the H-plane waveguide is analytically solved. The Fourier transform method is used to obtain the solution (57) in simple analytic series form. The numerical computations are performed to illustrate the behaviors of scattering in terms of the junction size and frequency. It is demonstrated that the T-junction with a shorting plunger may be used as an ideal power divider. It is also shown that the waveguide with two short-circuited junctions can be used as a notch filter with a very high Q. The reflection and transmission coefficients given by (68)-(71) are analytic closed-forms so that they are very efficient for numerical evaluation. The present approach may be easily

TABLE I
BEHAVIORS OF c_m, d_m, AND ENERGY CONSEVATION VERSUS m $(b/a = 1, d/a = 1, p = 0.2\lambda, q = \infty s = 1, \alpha = 0, k_1 b/\pi = 3.05)$

m	$\lvert c_m Y_q(-b)\rvert$	$\lvert d_m X_p(0)\rvert$	$\rho + \tau_1 + \tau_1$
1	0.142635	0.141627	1.52339
2	0.0811674	0.0467924	1.51798
3	0.599700	0.213364	1.00498
4	0.165912	0.107966	1.00604
5	0.0250421	0.0263598	0.995647
6	0.0410783	0.0354237	1.00000

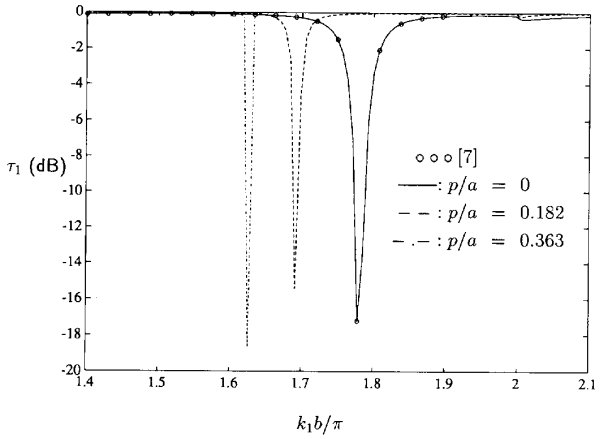

Fig. 4. Behaviors of Transmission (τ_1) Coefficient versus Normalized Frequency $(k_1 b/\pi)(b/a = 2.07, d/a = 1, q/a = 0.526, s = 1, \alpha = 0)$.

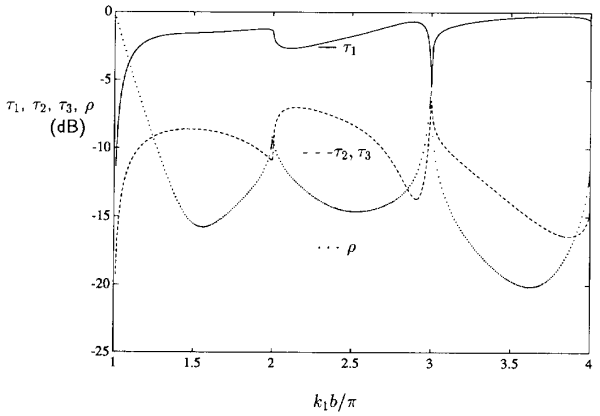

Fig. 5. Behaviors of Reflection (ρ) Transmission(τ_1 and τ_2) Coefficients versus Normalized Frequency $(k_1 b/\pi)(b/a = 2, d/a = 1, p = q = \infty, s = 1, \alpha = 0)$.

extended to the problem dealing with scattering from more than two junctions. The size of matrix and the computational amount for N-junction scattering problem will become N^2 times that of single-junction scattering.

REFERENCES

[1] M. Koshiba and M. Suzuki, "Application of the boundary-element method to waveguide discontinuities," *IEEE Trans. Microwave Theory Tech.*, vol. MTT-34, pp. 301–307, Feb. 1986.

[2] X. P. Liang, K. A. Zaki and A. E. Atia, "A rigorous three plane mode-matching technique for characterizing waveguide T-junctions and its application in multiplexer design," *IEEE Trans. Microwave Theory Tech.*, vol. 39, pp. 2138–2147, Dec. 1991.

[3] A. Widarta, S. Kuwanu, and K. Kokubun, "An analysis of transmission properties of rectangular waveguide T-junction," *Proc. 1992 IEICE Fall Conf. (Part 2)*, Tokyo, Inst. Tech., Sept. 27–30, 1992. p. 2-339 .

[4] N. Marcuvitz, *Waveguide Handbook*, Radiation Laboratory Series, vol. 10, New York: McGraw-Hill, 1951.

[5] K. H. Park and H. J. Eom, "An analytic series solution for H-plane waveguide T-junction," *IEEE Microwave and Guided Wave Letters*, vol. 3, no. 4, pp. 104–106, April 1993.

[6] ——, "An analytic series solution for E-plane T-junction in parallel-plate waveguide," *IEEE Trans. Microwave Theory Tech.*, vol. 42, pp. 356–358, Feb. 1994.

[7] T. Suga, Y. Yanagawa and F. Ishihara, "The mode conversion type bandstop filter in rectangular waveguide," *Proc. 1992 IEICE Fall Conf. (Part 2)*, Tokyo Inst. Tech., Sept. 27–30, 1992, p. 2-438.

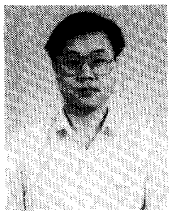

Jae W. Lee was born in Korea in 1970. He received the B.S. degree in electronic engineering from the Hanyang University, Seoul, Korea in 1992. He is now working toward the Ph.D. degree in electrical engineering at the Korea Advanced Institute of Science and Technology at Taejon, Korea, with an emphasis in electromagnetics.

Hyo Joon Eom received the B.S. degree in electronic engineering from Seoul National University, Korea, and the M.S. and Ph.D. degrees from the University of Kansas, Lawrence, in 1977 and 1982, respectively. From 1981 to 1984, he was a research associate at the Remote Sensing Laboratory of the University of Kansas. From 1984 to 1989, he was with the faculty of the Department of Electrical Engineering and Computer Science, University of Illinois at Chicago. He joined the Department of Electrical Engineering, Korea Advanced Institute of Science and Technology in 1989 as an associate professor. His research interests are radar remote sensing and wave scattering.